Eyewall and Rainband Eddy Forcing in Tropical Cyclone Intensification

Ping Zhu

Department of Earth & Environment

Florida International University

Bryce Tyner, Jun A. Zhang, Eric Aligo, Sundararaman Gopalakrishnan, Frank D. Marks, Avichal Mehra, Vijay Tallapragada

NOAA, HRD, EMC, NOAA

Outlines

1. A brief discussion of TC intensification by eyewall/rainband eddy forcing
2. A short review on our previous attempt to include eyewall/rainband in-cloud turbulent mixing in the HWRF PBL scheme.
3. Our recent progress on improving in-cloud turbulent mixing parameterization in HWRF.
4. Diagnosing the role of eddy forcing in TC intensification from HWRF output.
5. Summary

Azimuthal-mean tangential wind budget equation in a cylindrical coordinate

$$\frac{\partial \bar{v}}{\partial t}+\bar{u}\frac{\partial \bar{v}}{\partial r}+\bar{w}\frac{\partial \bar{v}}{\partial z}=\bar{u}\left(f+\frac{\bar{v}}{r}\right)+F_{\lambda}+F_{sgs\_\lambda},\ \text{where}$$

$$F_{\lambda}=-\overline{u'\frac{\partial v'}{\partial r}}-\overline{v'\frac{\partial v'}{r\partial \lambda}}-\overline{w'\frac{\partial v'}{\partial z}}-\frac{\overline{u'v'}}{r}$$: model-resolved eddy forcing

F_{sgs_λ} : parameterized sub-grid scale (SGS) eddy forcing

$$\frac{D\bar{M}}{Dt}=\frac{\partial \bar{M}}{\partial t}+\bar{u}\frac{\partial \bar{M}}{\partial r}+\bar{w}\frac{\partial \bar{M}}{\partial z}=r\left(F_{\lambda}+F_{sgs_{\lambda}}\right),$$

where $\bar{M}=r\bar{\tilde{v}}+\frac{1}{2}fr^2$ is the azimuthal-mean absolute angular momentum

While higher model grid resolution allows the eddy forcing to be better resolved during the simulation, the uncertainty arises from the parametrical determination of SGS eddy processes.

$$\frac{D\bar{M}}{Dt} = r\left(F_\lambda + F_{sgs_\lambda}\right),$$

The importance of boundary layer turbulent transport to TC evolution has long been recognized and is a focus of current research. But the importance of SGS eddy forcing above the boundary layer has been largely overlooked.

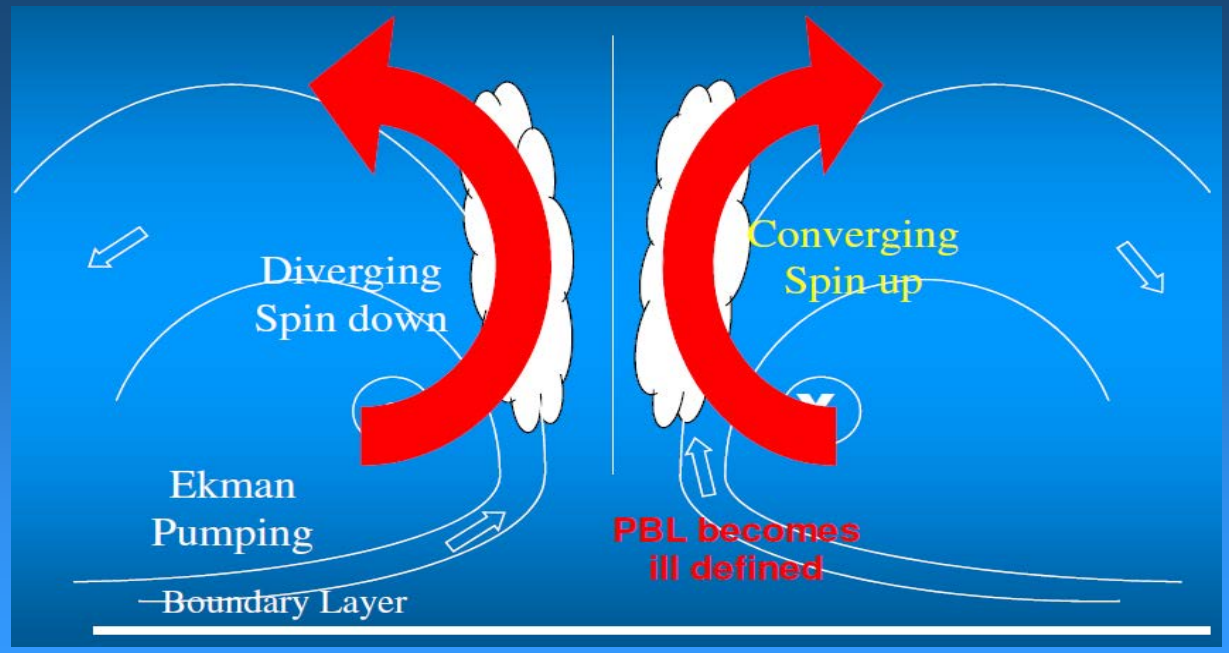

- It is overshadowed by the critical role of radial inflow and surface latent heating in maintaining and intensifying a TC.
- Lack of observations largely limits our understanding of the aloft in-cloud turbulent mixing processes.
- For deep convection, the focus is on the cumulus parameterization.
- Historically, all turbulent mixing schemes used today were originally developed to represent turbulent processes in the PBL.

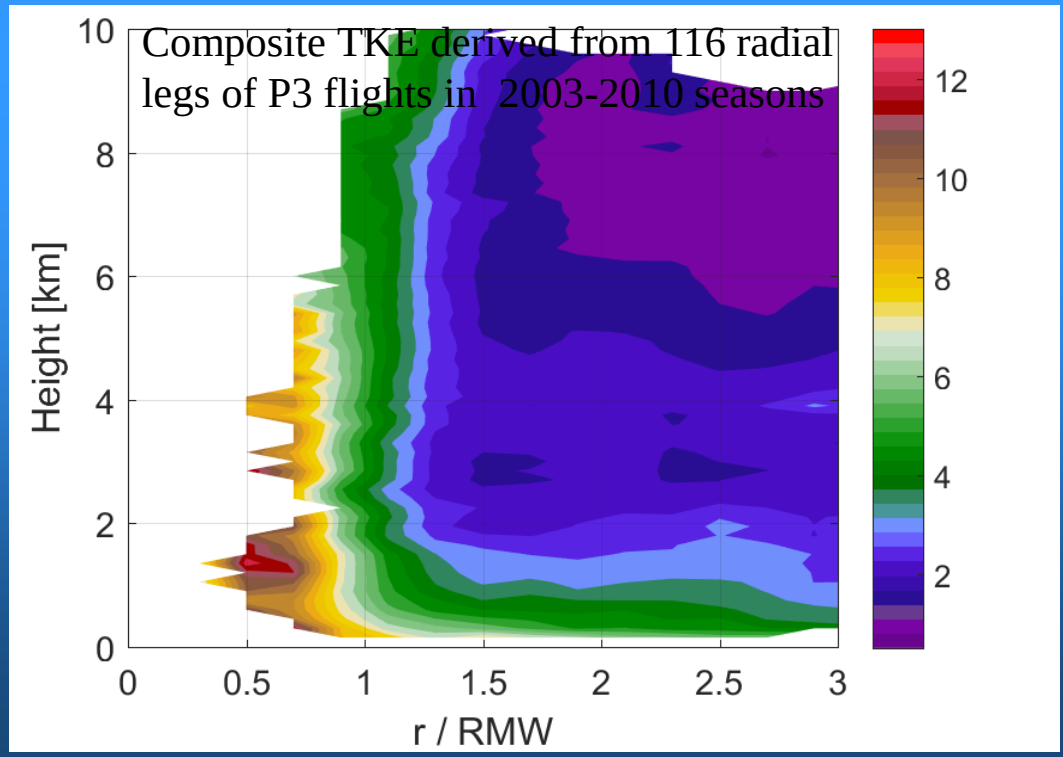

Eddy exchange coefficients from a HWRF simulation of Hurricane Jimena (2015) at different altitudes at 12:00 UTC, 28 August, 2015

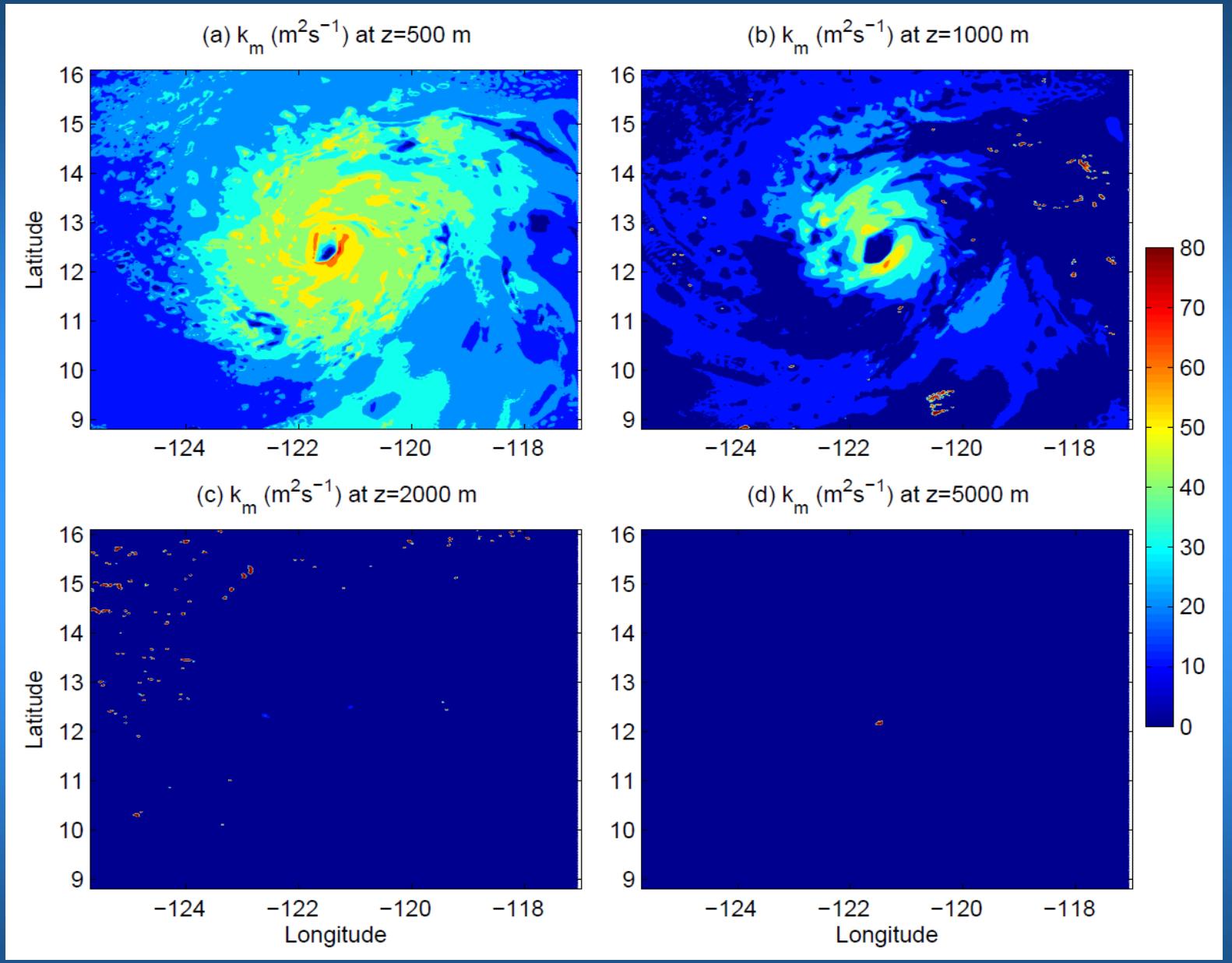

We hypothesize that lack of appropriate SGS eddy forcing associated with eyewell/rainband convection above the PBL is one of the culprits for the intensity forecast failure in many cases.

HWRF PBL scheme is a typical K-closure scheme

$$K_m = \kappa \frac{u_*}{\phi_m} \alpha z (1 - \frac{z}{h})^2, \qquad z<h, \qquad h=Ri_{cr} \frac{\theta_{va}|U(h)|^2}{g[\theta_v(h)-\theta_s]}$$

In reality, there is no physical interface that separates the turbulence in the eyewall generated by the surface and cloud processes. From the nature of turbulent mixing, it is more logical to parameterize the turbulence in the eyewall and rainbands based on the integrated "Turbulent Layer (TL)".

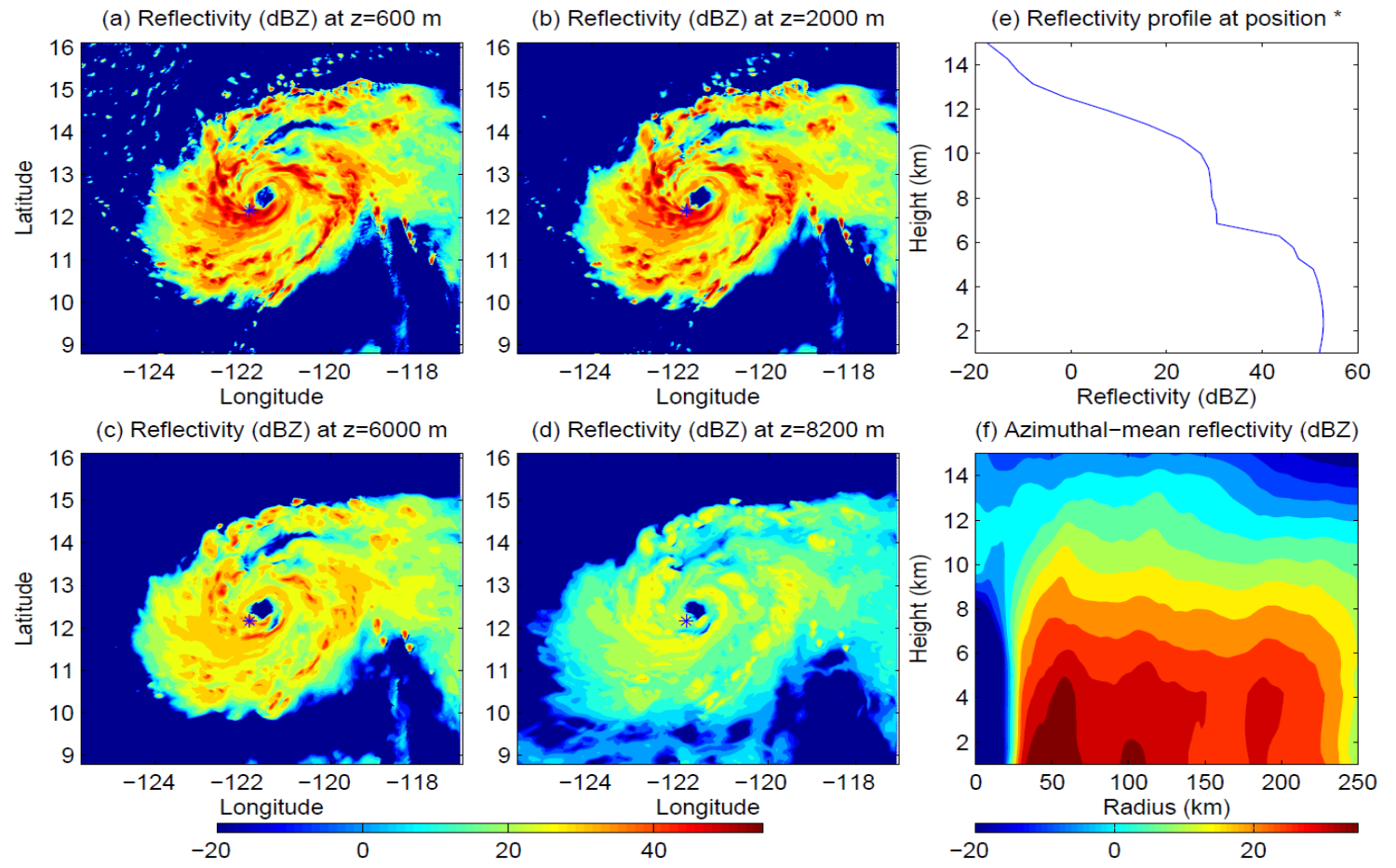

12:00 UTC, 28 August, 2015

Eddy exchange coefficients from the same HWRF simulation of Jimena (2015) but with the inclusion of in-cloud turbulent mixing parameterization (12:00 UTC, 28 August, 2015)

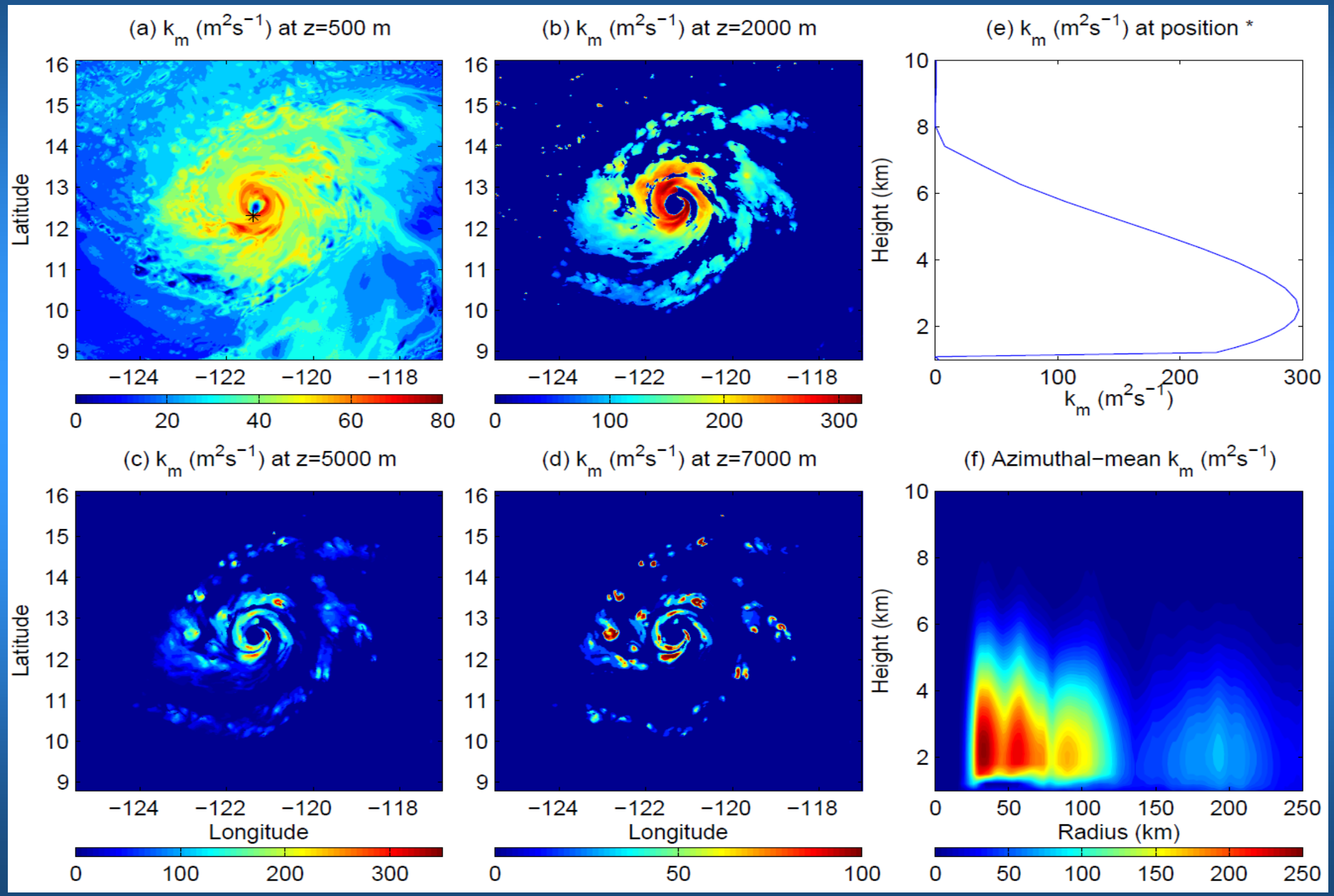

Comparison of HWRF simulated storm intensity and track of Jimena (2015) with the best track data

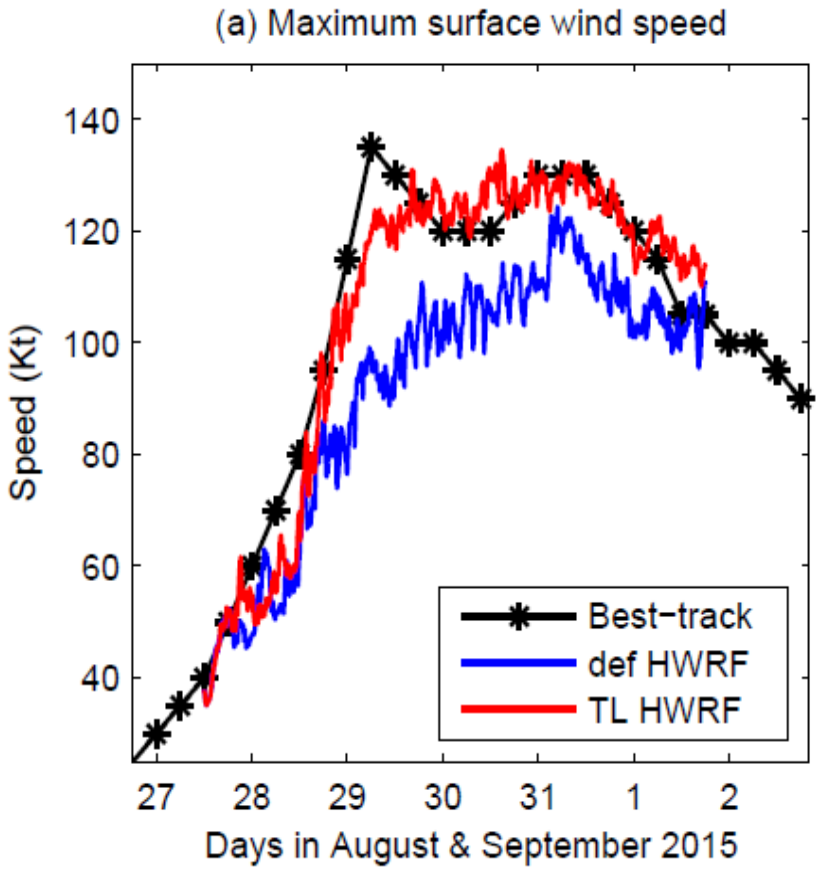

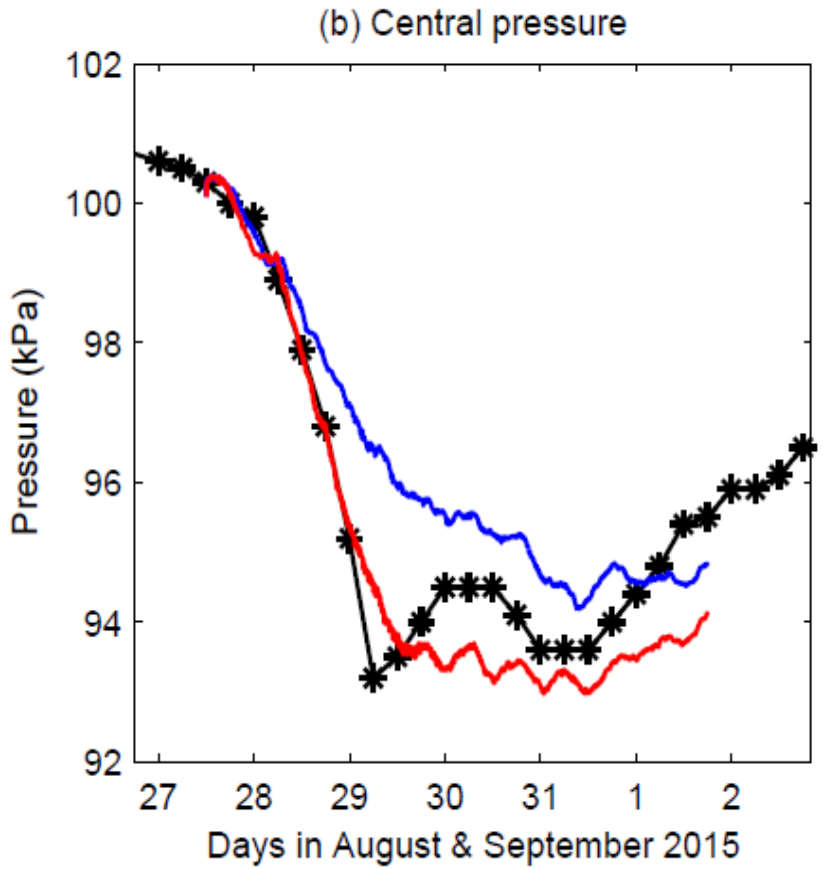

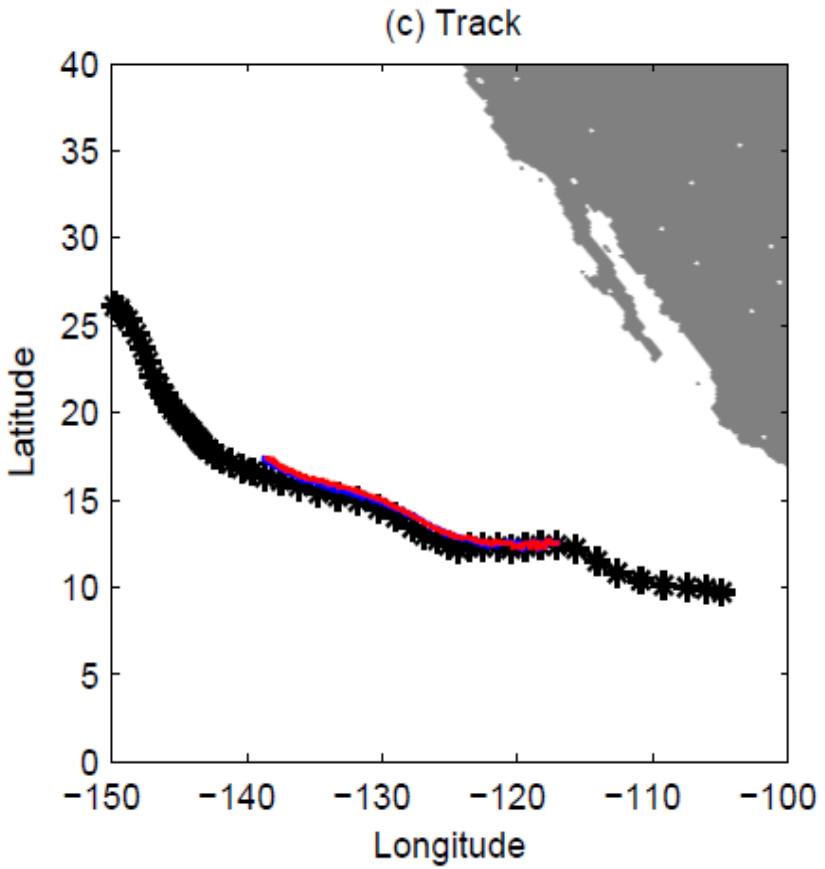

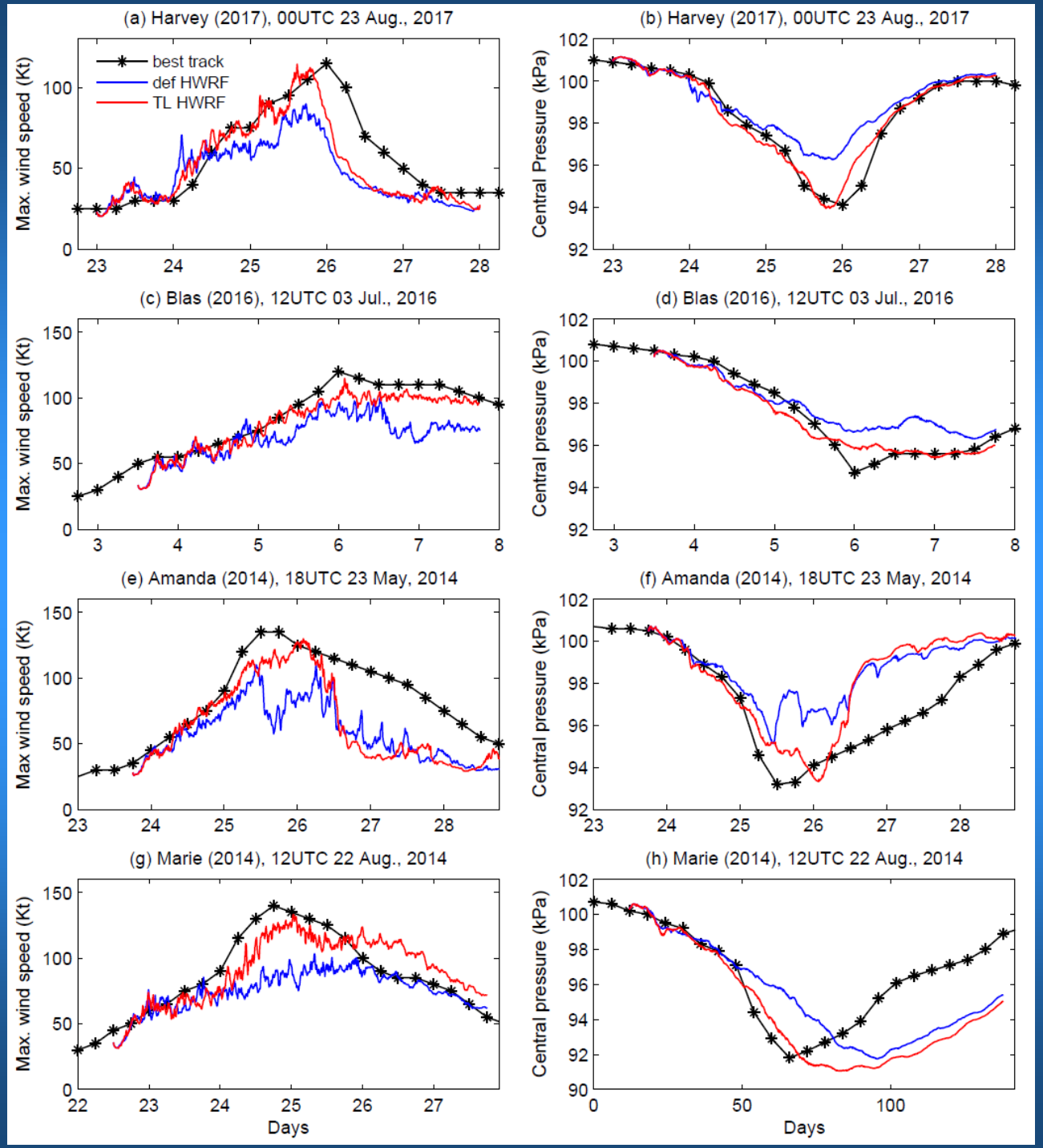

$$K_m = \kappa \frac{u_*}{\phi_m} \alpha z (1 - \frac{z}{h})^2,$$
$$z<h$$

In the default HWRF PBL scheme, the turbulent eddy exchange coefficient above the diagnosed boundary layer height is calculated by,

$$K_{m,t} = l^2 f_{m,t}(Ri_g)\sqrt{\left|\frac{\partial \bar{u}}{\partial z}\right|^2 + \left|\frac{\partial \bar{v}}{\partial z}\right|^2}, \qquad z \geq h, \qquad l \text{ is the mixing length.}$$

$f_{m,t}(Ri_g)$ is a stability function of gradient Richardson number.

$$Ri_g = N^2 / \left(\left|\frac{\partial \bar{u}}{\partial z}\right|^2 + \left|\frac{\partial \bar{v}}{\partial z}\right|^2\right),$$

Brunt-Vaisala frequency, $N^2 = \frac{g}{\theta_0}\frac{\partial \overline{\theta_v}}{\partial z}$ (A very poor estimate in clouds!)

This method is also adapted by the YSU PBL scheme to treat turbulent mixing above the boundary layer. But they included the cloud effects on Brunt-Vaisala frequency by reducing stability using the following formula,

$$N_c^2 = (1+B)\left[N^2 - \frac{g^2}{C_p T}\left(\frac{A-B}{1+A}\right)\right], \quad A = \frac{L^2 q_s}{C_p R_v T^2}, \quad B = \frac{L q_s}{RT}.$$

For $T \propto [300K, 240K] \rightarrow A \propto [3.69,\ 0.06], B \propto [0.71,\ 0.009]$, $\frac{g^2}{C_p T}\left(\frac{A-B}{1+A}\right) \propto [2.02,\ 0.19] \times 10^{-4}$.

In the eyewall, $N^2 \propto [\pm 0, 1 \times 10^{-4}]$ → This equation significantly over-reduces stability!

Using parcel theory, acceleration $a = -g\frac{\rho_p - \rho_e}{\rho_e} = N_m^2\delta$, Durran & Klemp (1982) showed for saturated atmosphere,

$$N_m^2 \approx g\left\{\frac{1+B}{1+A}\left(\frac{d\ln\theta}{dz} + \frac{L}{C_pT}\frac{dq_s}{dz}\right) - \frac{dq_t}{dz}\right\}$$

$$\frac{dq_s}{dz} = \left(1 + \frac{q_s}{\varepsilon}\right)\left(\frac{Lq_s}{R_vT^2}\frac{dT}{dz} - \frac{q_s}{p}\frac{dp}{dz}\right).$$

$$N_m^2 = g\left\{\frac{1+B}{1+A}\left[\frac{d\ln\theta}{dz} + \frac{L}{C_pT}\left(1 + \frac{q_s}{\varepsilon}\right)\left(\frac{Lq_s}{R_vT^2}\frac{dT}{dz} - \frac{q_s}{p}\frac{dp}{dz}\right)\right] - \frac{dq_t}{dz}\right\}, \quad \frac{dp}{dz} = -\rho g$$

YSU made a couple of inappropriate assumptions:

(1), they dropped $\frac{dq_t}{dz}$. $\frac{dq_t}{dz} = \frac{dq_s}{dz} + \frac{dq_c}{dz}$, $N_m^2 = g\left\{\left(\frac{1+B}{1+A}\right)\left[\frac{d\ln\theta}{dz} + \left(\frac{L}{C_pT} - \frac{1+A}{1+B}\right)\frac{dq_s}{dz}\right] - \frac{dq_c}{dz}\right\}$.

(2), they assumed $\frac{dT}{dz} = -\frac{g}{C_p}$, apparently incorrect in the clouds!

$$\longrightarrow N_m^2 \approx (1+B)\left[N^2 - \frac{g^2}{C_pT}\left(\frac{A-B}{1+A}\right)\right] \text{ (YSU formula)}$$

Because of significantly over-reduced Brunt-Vaisala frequency in clouds, it generates unrealistically large $K_{m,t}$. What YSU did is to artificially reduce $K_{m,t}$ by averaging in-cloud $K_{m,t}^{cld}$ and entrainment $K_{m,t}^{ent}$,

$$K_{m,t} = \left(K_{m,t}^{cld} \cdot K_{m,t}^{ent}\right)^{1/2}$$

$$K_{m,t}^{ent} = Pr_{m,t} \frac{-\overline{w'\theta_v'}_h}{(\partial\theta_v/\partial z)_h} \exp\left[-\frac{(z-h)^2}{\delta^2}\right], \qquad \frac{\delta}{h} \approx 0.02$$

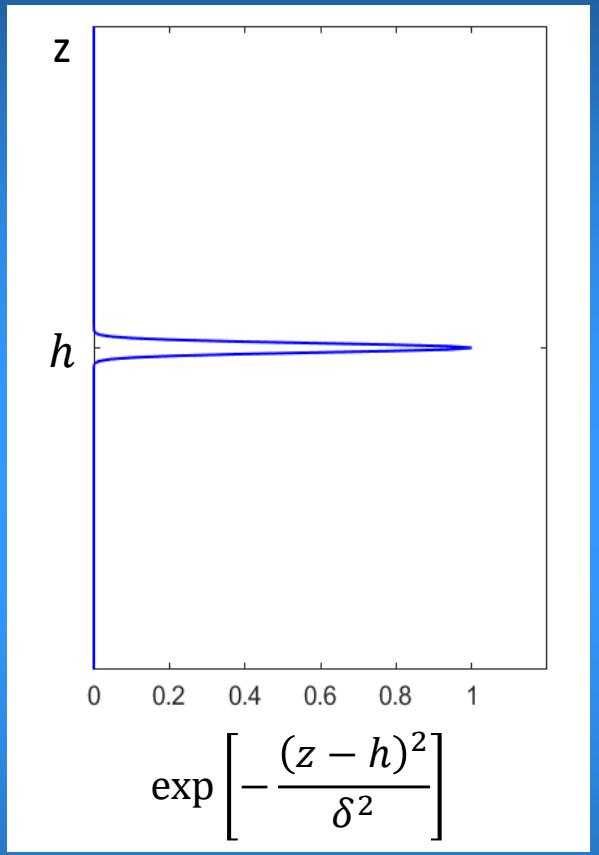

In HWRF, we recalculated Brunt-Vaisala frequency using,

$$N_m^2 = g\left\{\frac{1+B}{1+A}\left[\frac{d\ln\theta}{dz} + \frac{L}{C_pT}\left(1+\frac{q_s}{\varepsilon}\right)\left(\frac{Lq_s}{R_vT^2}\frac{dT}{dz} + \frac{q_s g}{RT_v}\right)\right] - \frac{dq_t}{dz}\right\}$$

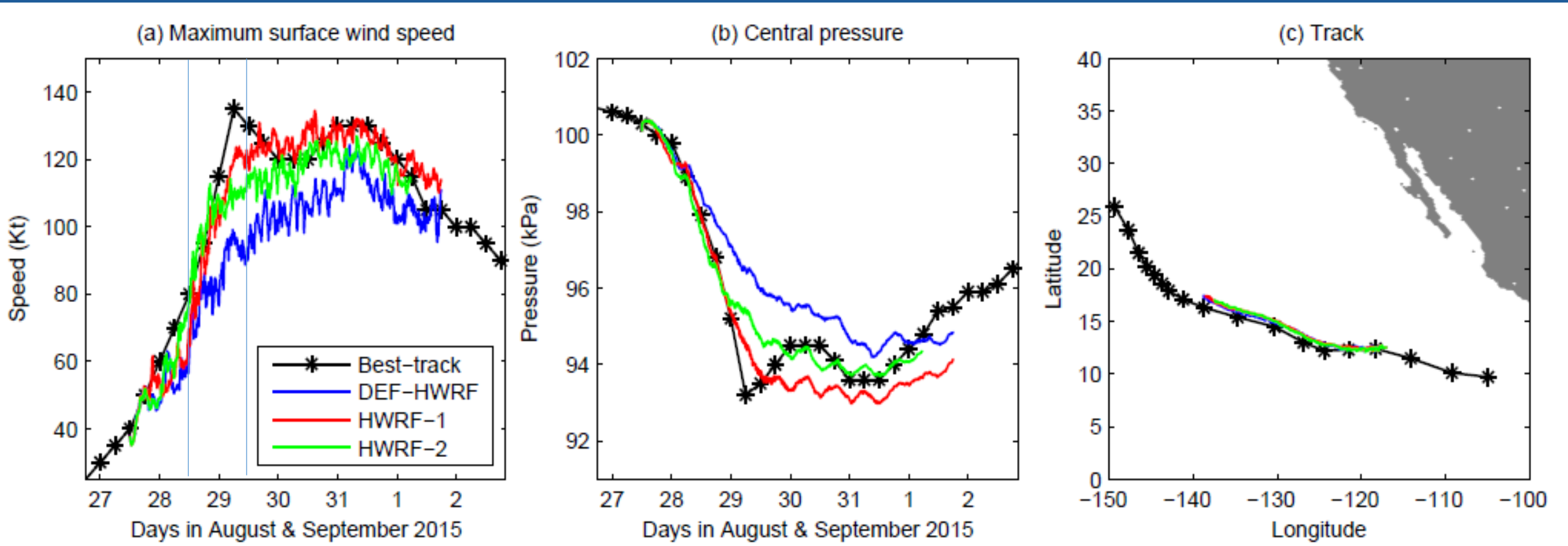

HWRF-1: parameterization of in-cloud turbulent mixing based on the TL concept

HWRF-2: parameterization of in-cloud turbulent mixing by recalculating N^2 in clouds

Comparison of TC inner-core structure of Jimena (2015) between satellite observations and two HWRF simulations right before Jimena's RI.

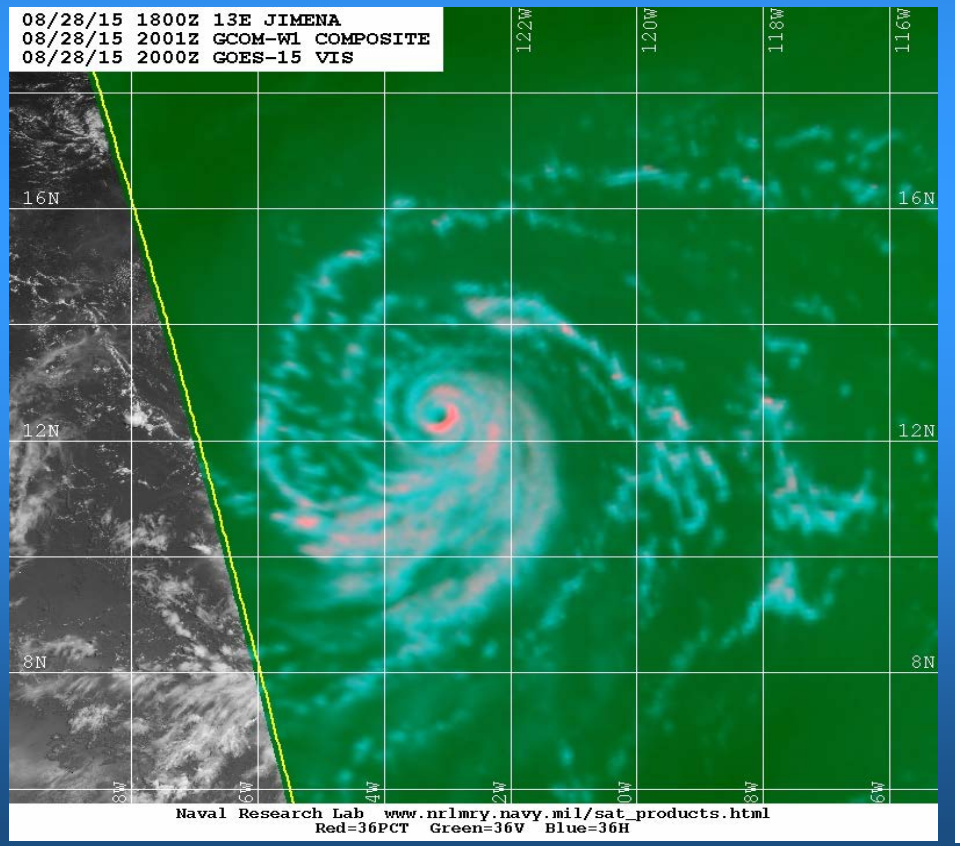

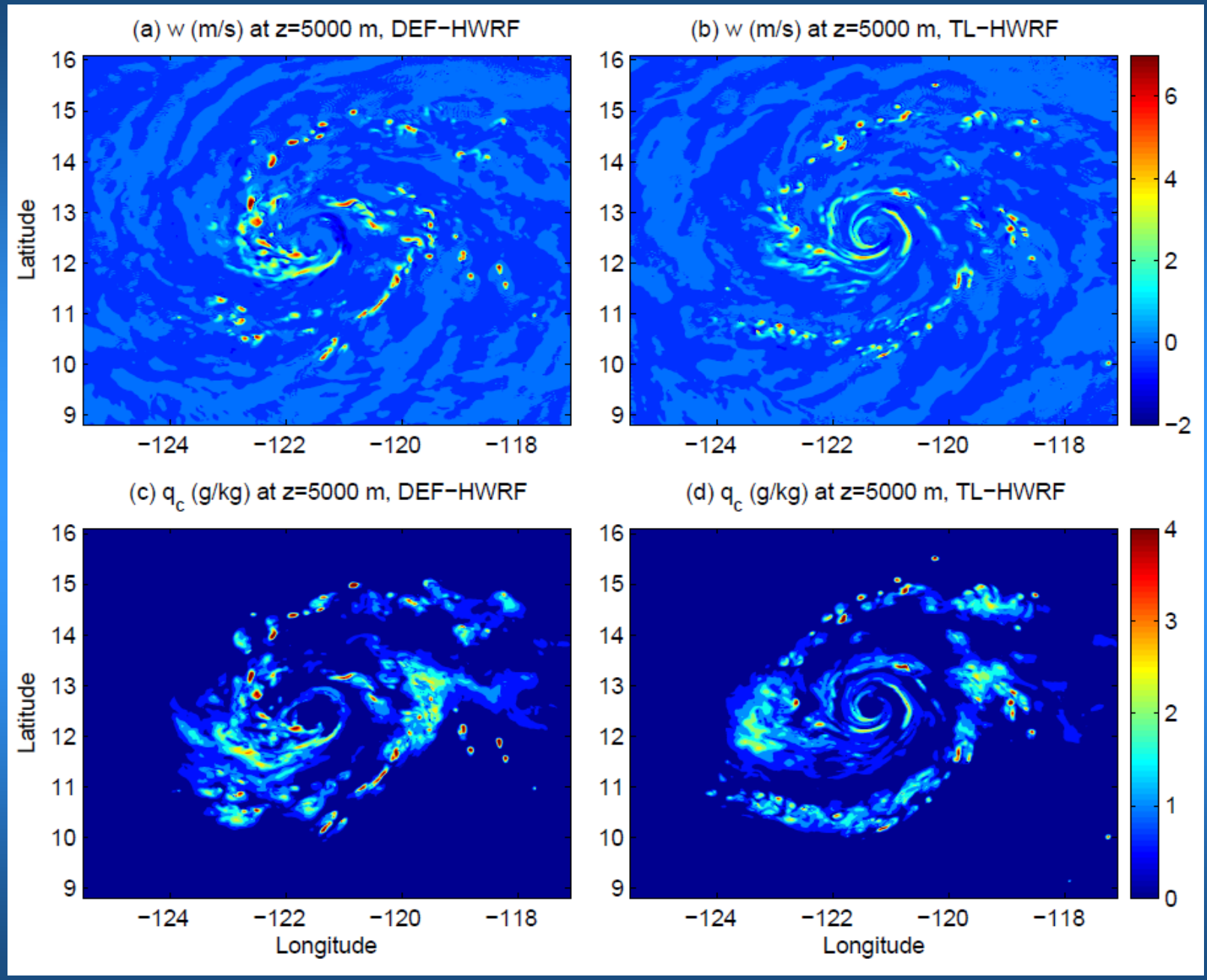

20:00 UTC August 28, 2015

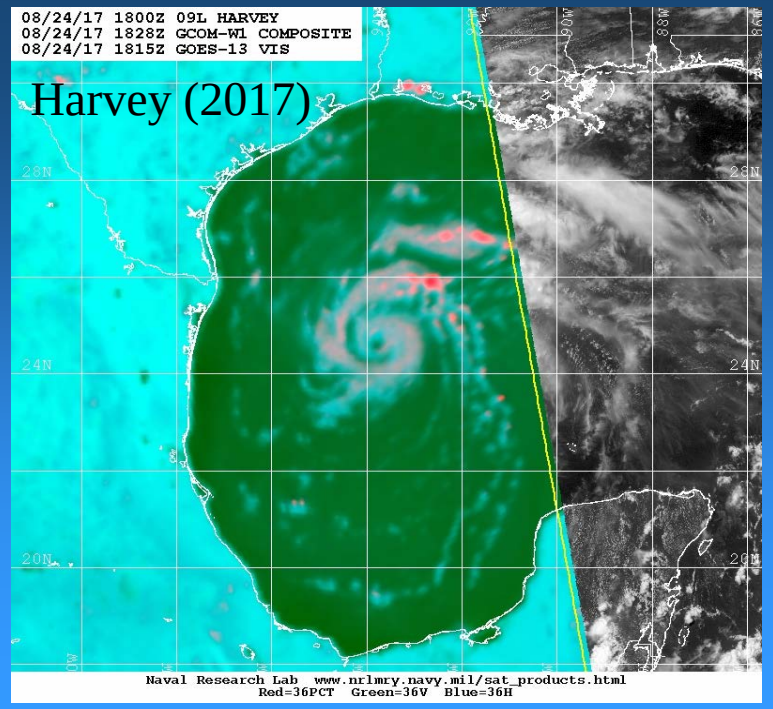
08/24/17 1800Z 09L HARVEY
08/24/17 1828Z GCOM-W1 COMPOSITE
08/24/17 1815Z GOES-13 VIS
Harvey (2017)
Naval Research Lab www.nrlmry.navy.mil/sat_products.html
Red=36PCT Green=36V Blue=36H

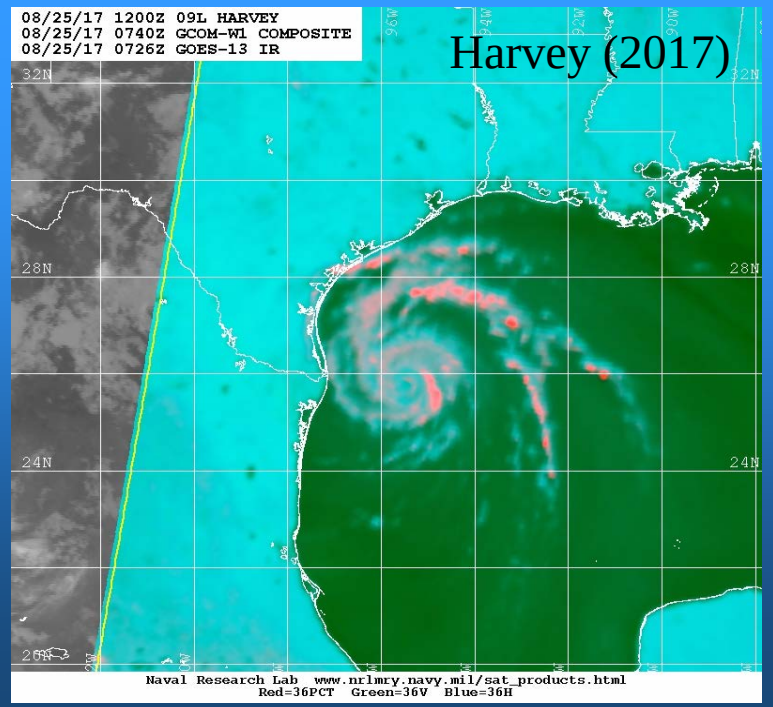
08/25/17 1200Z 09L HARVEY
08/25/17 0740Z GCOM-W1 COMPOSITE
08/25/17 0726Z GOES-13 IR
Harvey (2017)
Naval Research Lab www.nrlmry.navy.mil/sat_products.html
Red=36PCT Green=36V Blue=36H

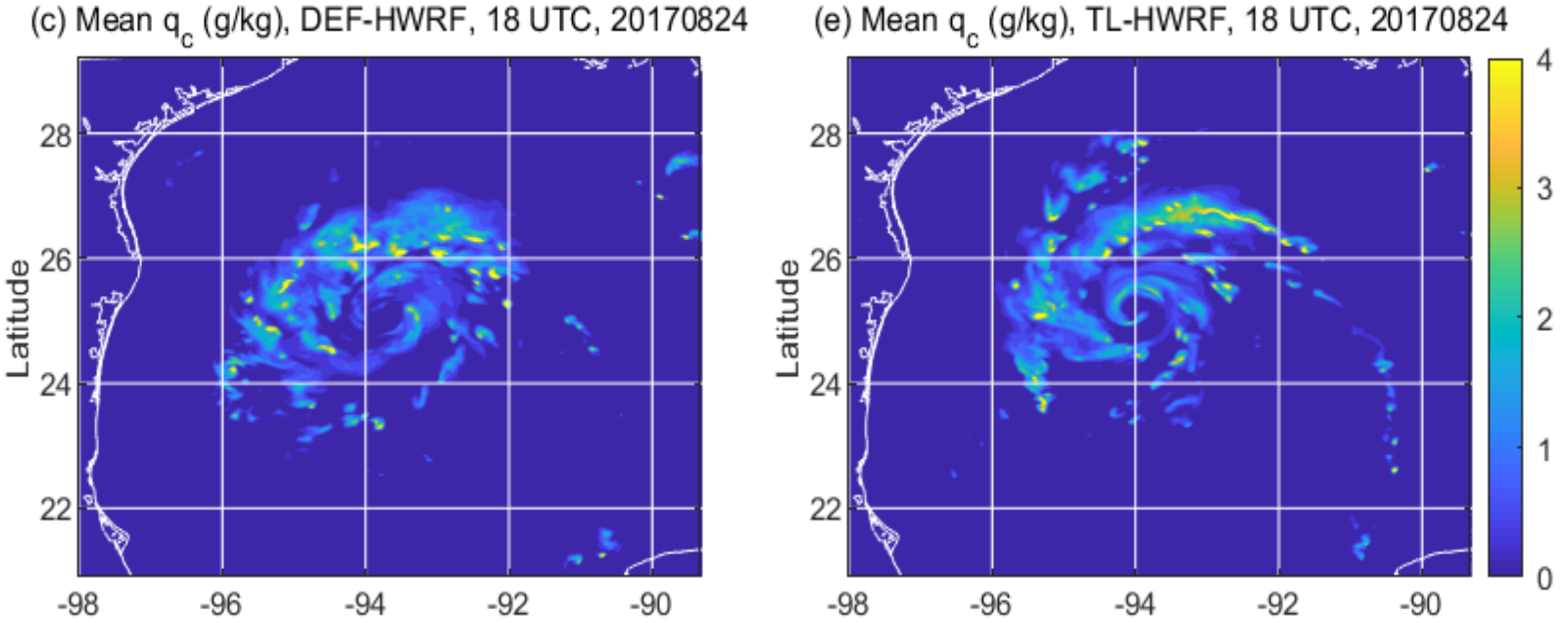
(c) Mean q_c (g/kg), DEF-HWRF, 18 UTC, 20170824
(e) Mean q_c (g/kg), TL-HWRF, 18 UTC, 20170824
Latitude
Longitude

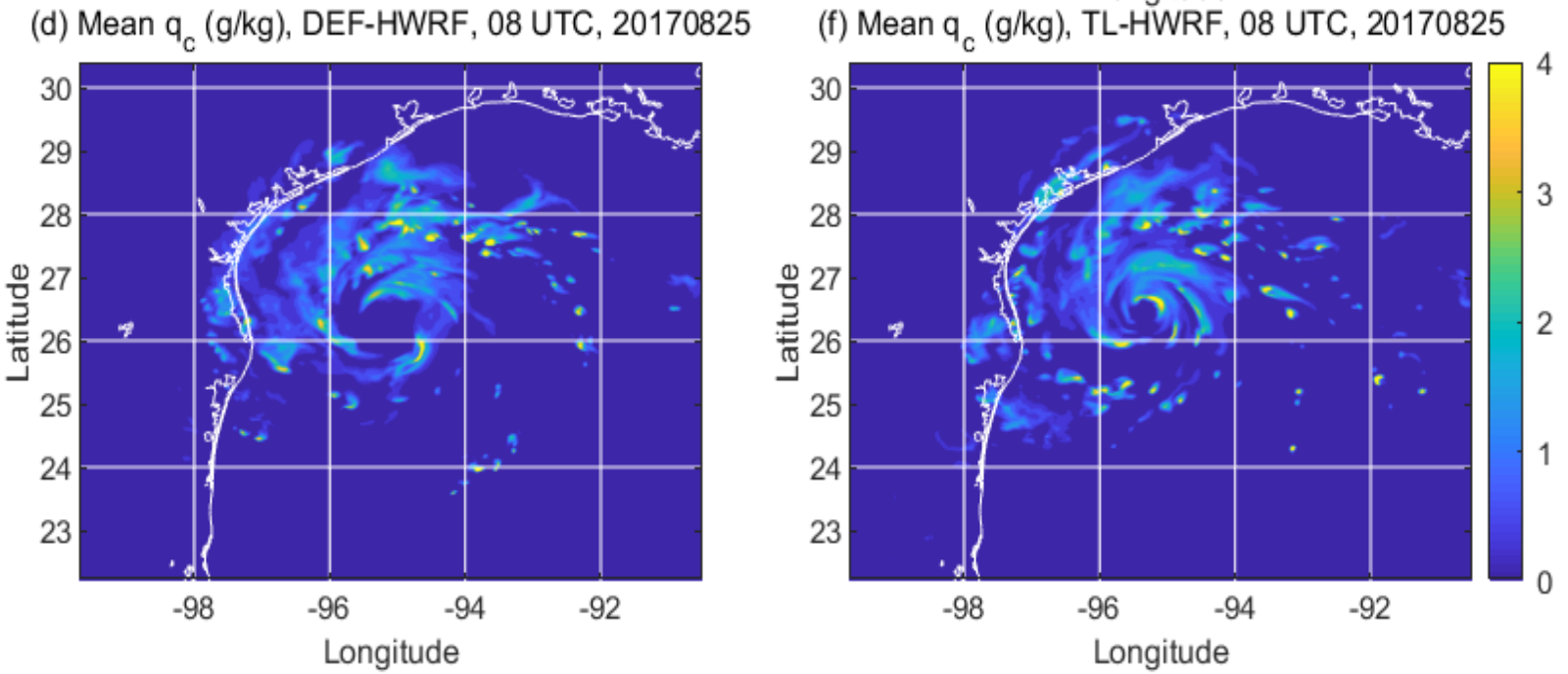
(d) Mean q_c (g/kg), DEF-HWRF, 08 UTC, 20170825
(f) Mean q_c (g/kg), TL-HWRF, 08 UTC, 20170825
Latitude
Longitude

Azimuthal-mean radius-height structure of Jimena (2015) simulated by HWRF averaged over the RI period from 12:00 UTC 08/28 to 06 UTC 08/29, 2015.

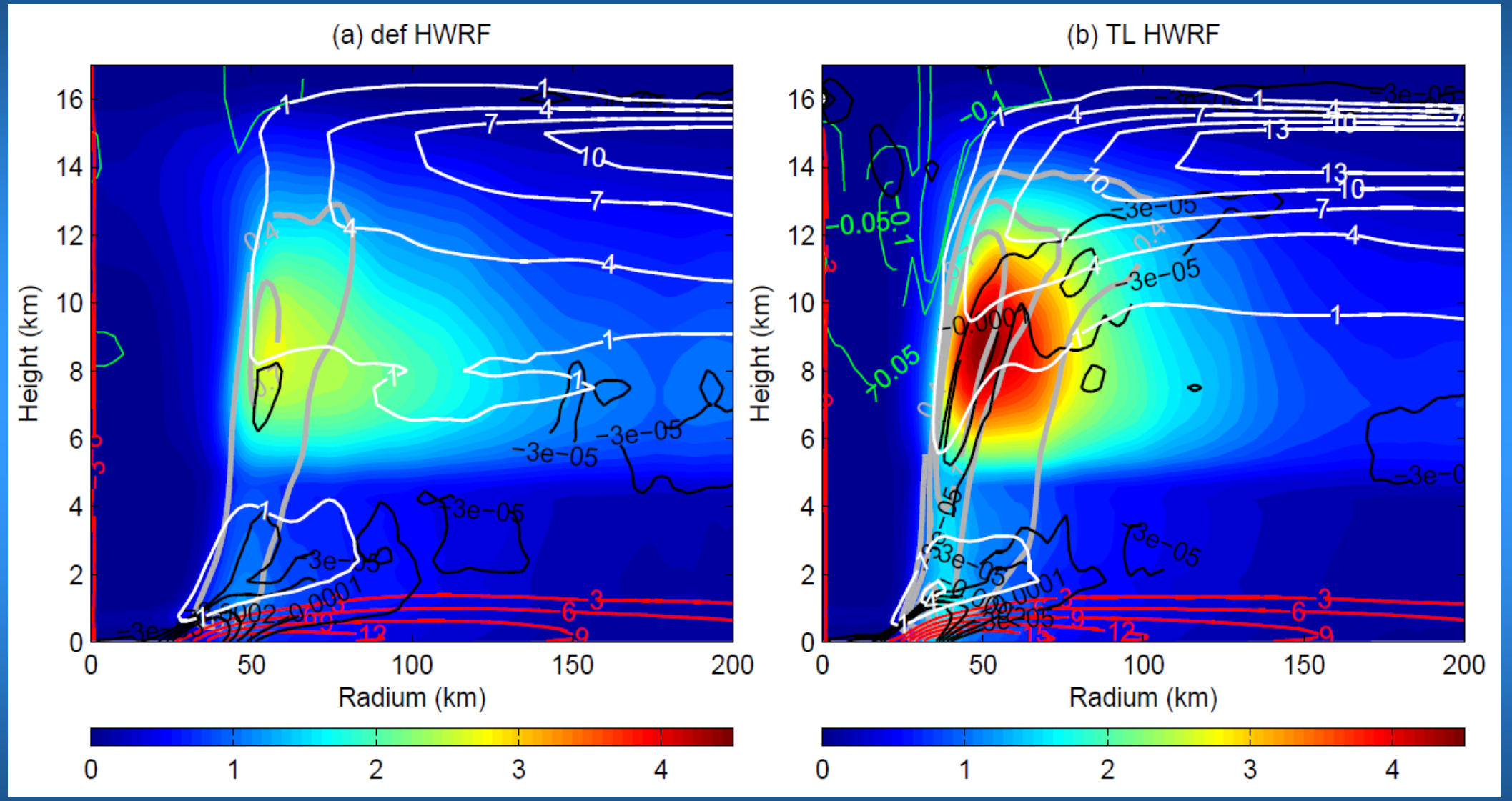

Hydrometeor mixing ration (color shades), updrafts (gray contours), downdraft (green contours), radial inflow (red contours), and convergence of radial flow (black contours)

Budget analyses

$$\frac{\partial \bar{v}}{\partial t} = -\bar{u}\frac{\partial \bar{v}}{\partial r} - \bar{w}\frac{\partial \bar{v}}{\partial z} - \bar{u}\left(f + \frac{\bar{v}}{r}\right) + F_\lambda + F_{sgs_\lambda}, \qquad F_\lambda = -\overline{u'\frac{\partial v'}{\partial r}} - \overline{v'\frac{\partial v'}{r\partial \lambda}} - \overline{w'\frac{\partial v'}{\partial z}} - \frac{\overline{u'v'}}{r}.$$

F_{sgs_λ}

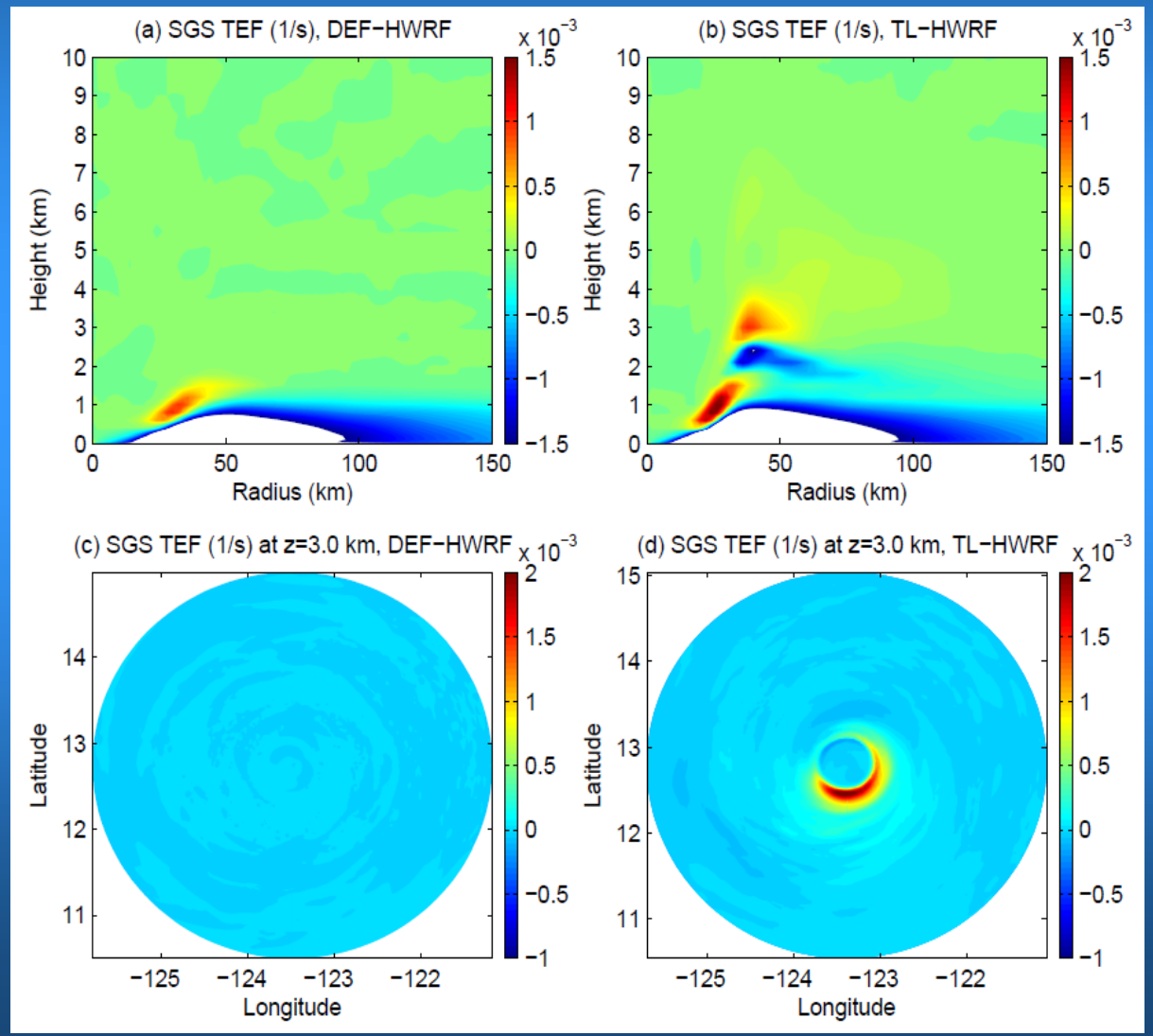

F_λ

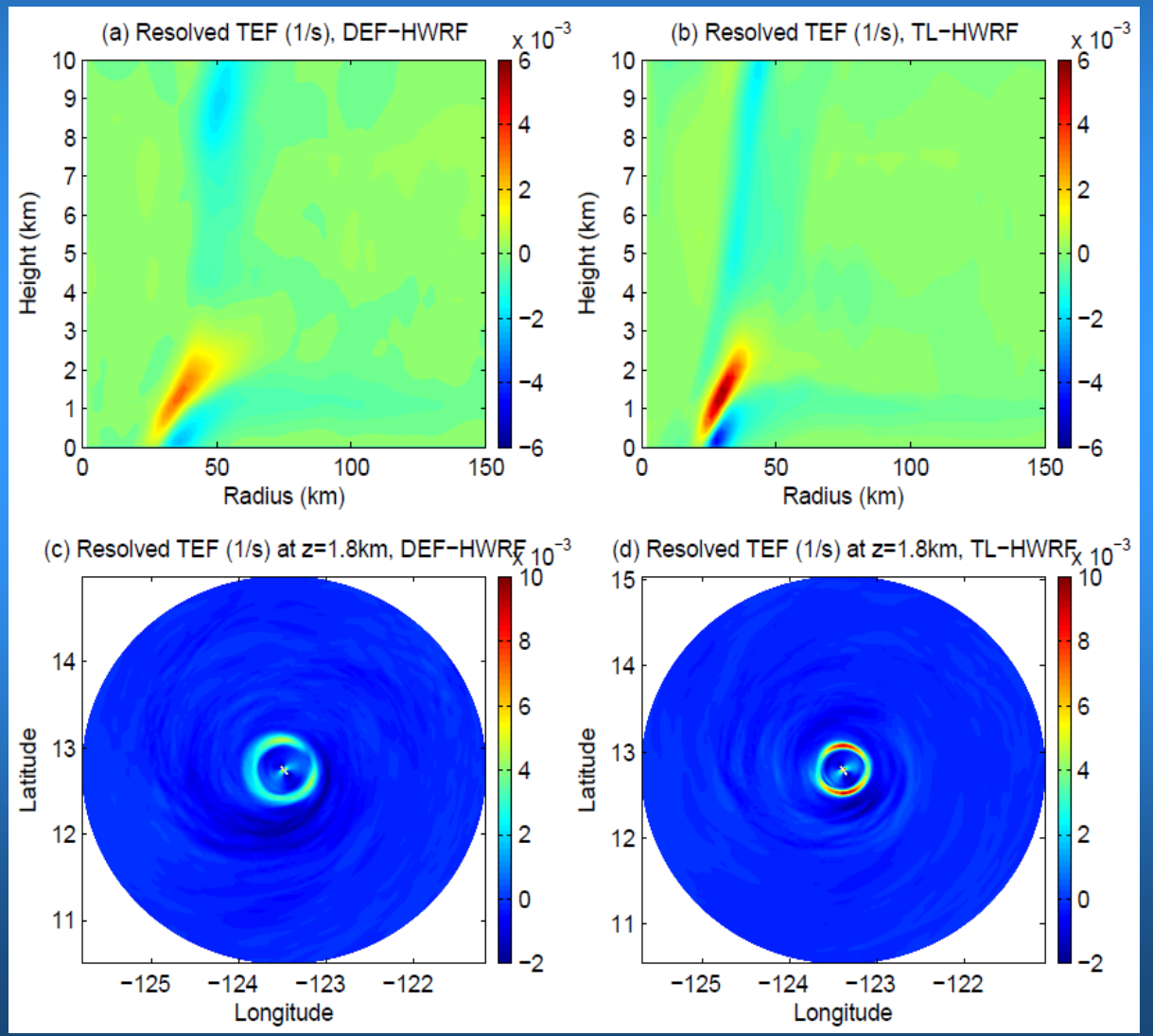

$$-\bar{u}\frac{\partial \bar{v}}{\partial r} - \bar{w}\frac{\partial \bar{v}}{\partial z} - \bar{u}\left(f + \frac{\bar{v}}{r}\right).$$

$$F_\lambda + F_{sgs_\lambda}$$

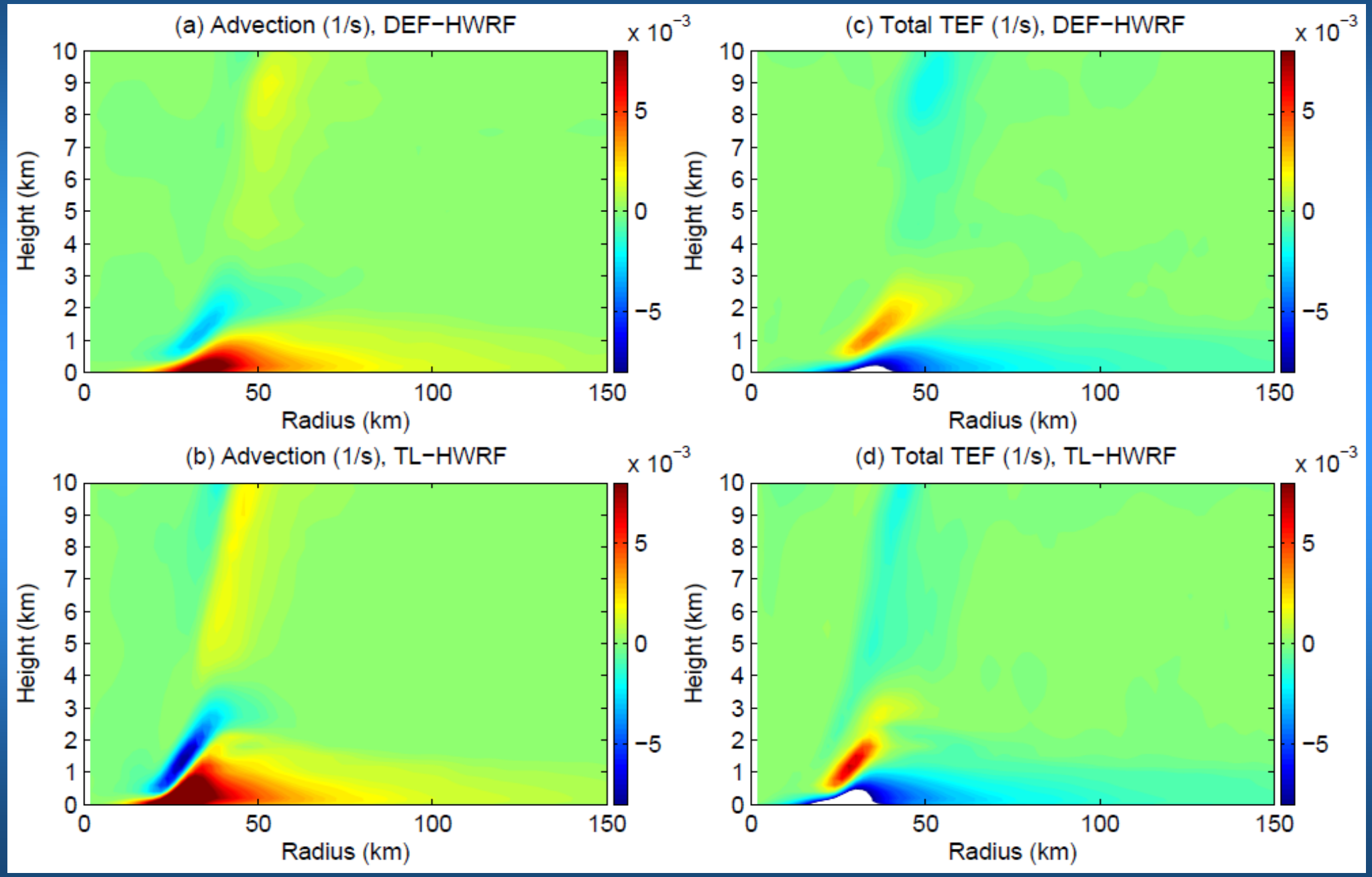

$$\frac{\partial \bar{u}}{\partial t} + \bar{u}\frac{\partial \bar{u}}{\partial r} + \bar{w}\frac{\partial \bar{u}}{\partial z} - C = -\frac{1}{\bar{\rho}}\frac{\partial \bar{p}}{\partial r} + F_r + F_{sgs\_r}, \qquad C = \frac{\bar{v}^2}{r} + f\bar{v}, \qquad F_r = -\overline{u'\frac{\partial u'}{\partial r}} - \overline{v'\frac{\partial u'}{r\partial \lambda}} - \overline{w'\frac{\partial u'}{\partial z}} + \frac{\overline{v'^2}}{r}$$

$$\frac{\partial \bar{w}}{\partial t} + \bar{u}\frac{\partial \bar{w}}{\partial r} + \bar{w}\frac{\partial \bar{w}}{\partial z} = -\frac{1}{\bar{\rho}}\frac{\partial \bar{p}}{\partial z} - g + F_w + F_{sgs\_w}, \qquad F_w = -\overline{u'\frac{\partial w'}{\partial r}} - \overline{v'\frac{\partial w'}{r\partial \lambda}} - \overline{w'\frac{\partial w'}{\partial z}}$$

$$NRF = C - \frac{1}{\bar{\rho}}\frac{\partial \bar{p}}{\partial r} \qquad NVF = -\frac{1}{\bar{\rho}}\frac{\partial \bar{p}}{\partial z} - g$$

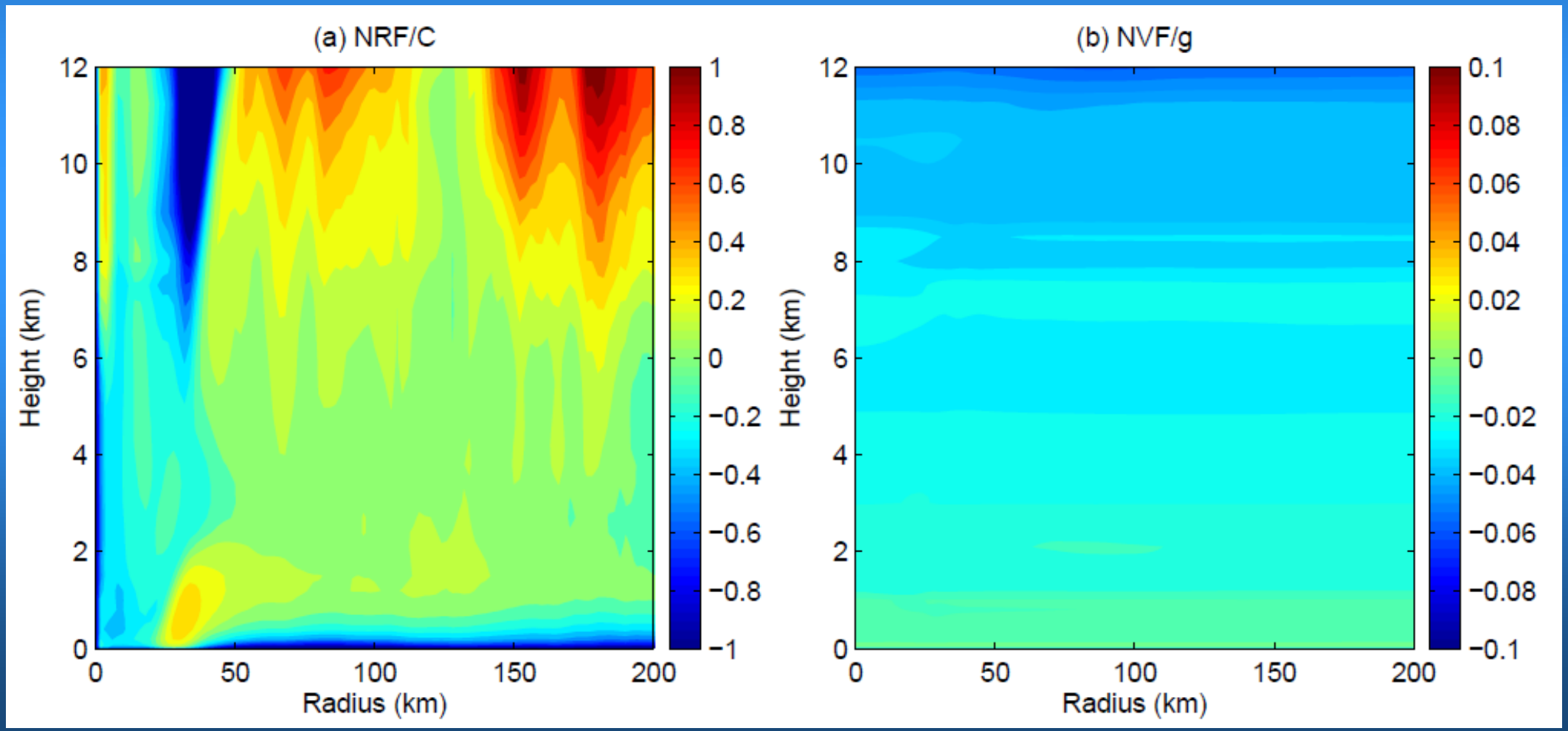

$$F_r = -\overline{u'\frac{\partial u'}{\partial r}} - \overline{v'\frac{\partial u'}{r\partial \lambda}} - \overline{w'\frac{\partial u'}{\partial z}} + \frac{\overline{v'^2}}{r}$$

F_{sgs_r}

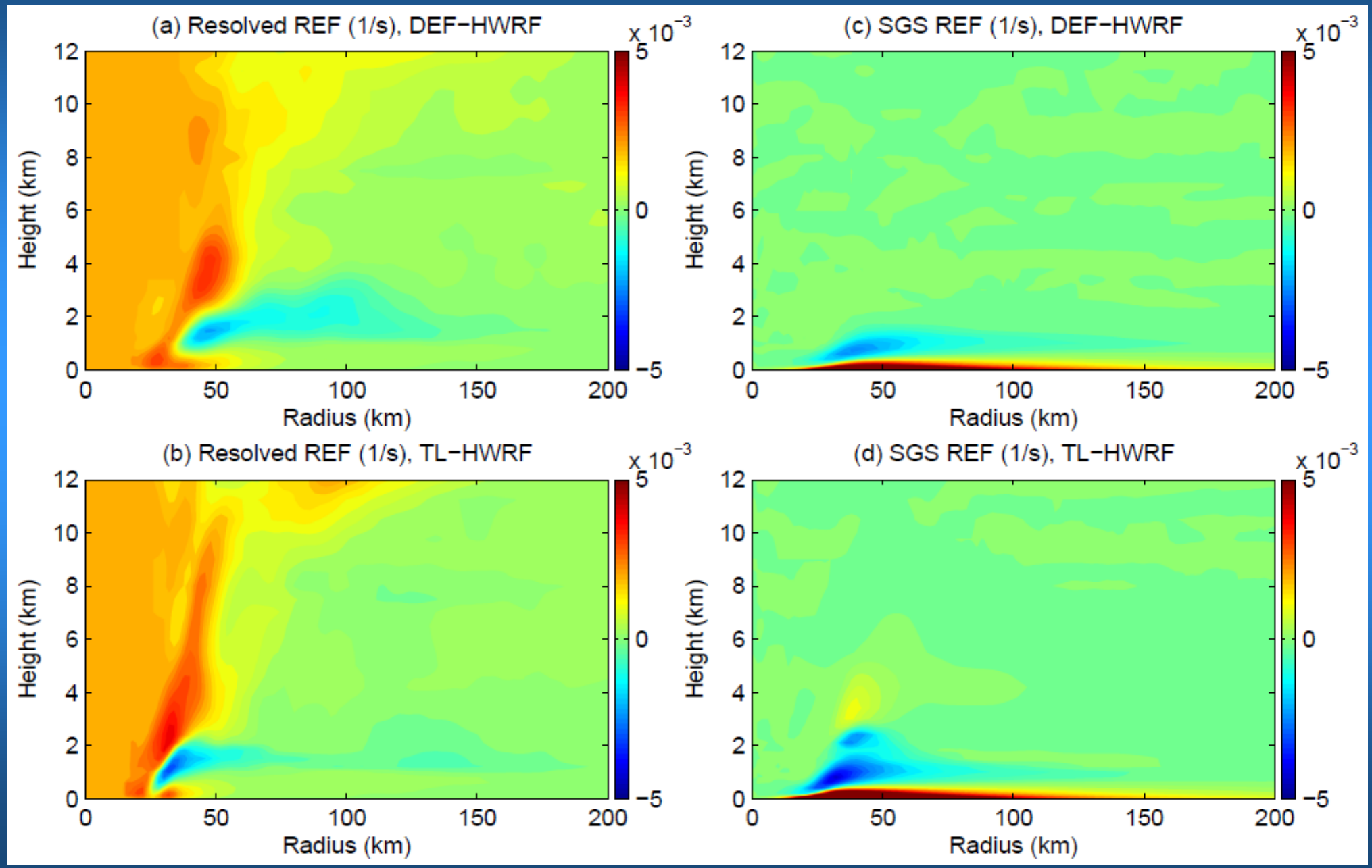

$$-\bar{u}\frac{\partial \bar{u}}{\partial r} - \bar{w}\frac{\partial \bar{u}}{\partial z}$$

$$F_r + F_{sgs\_r}$$

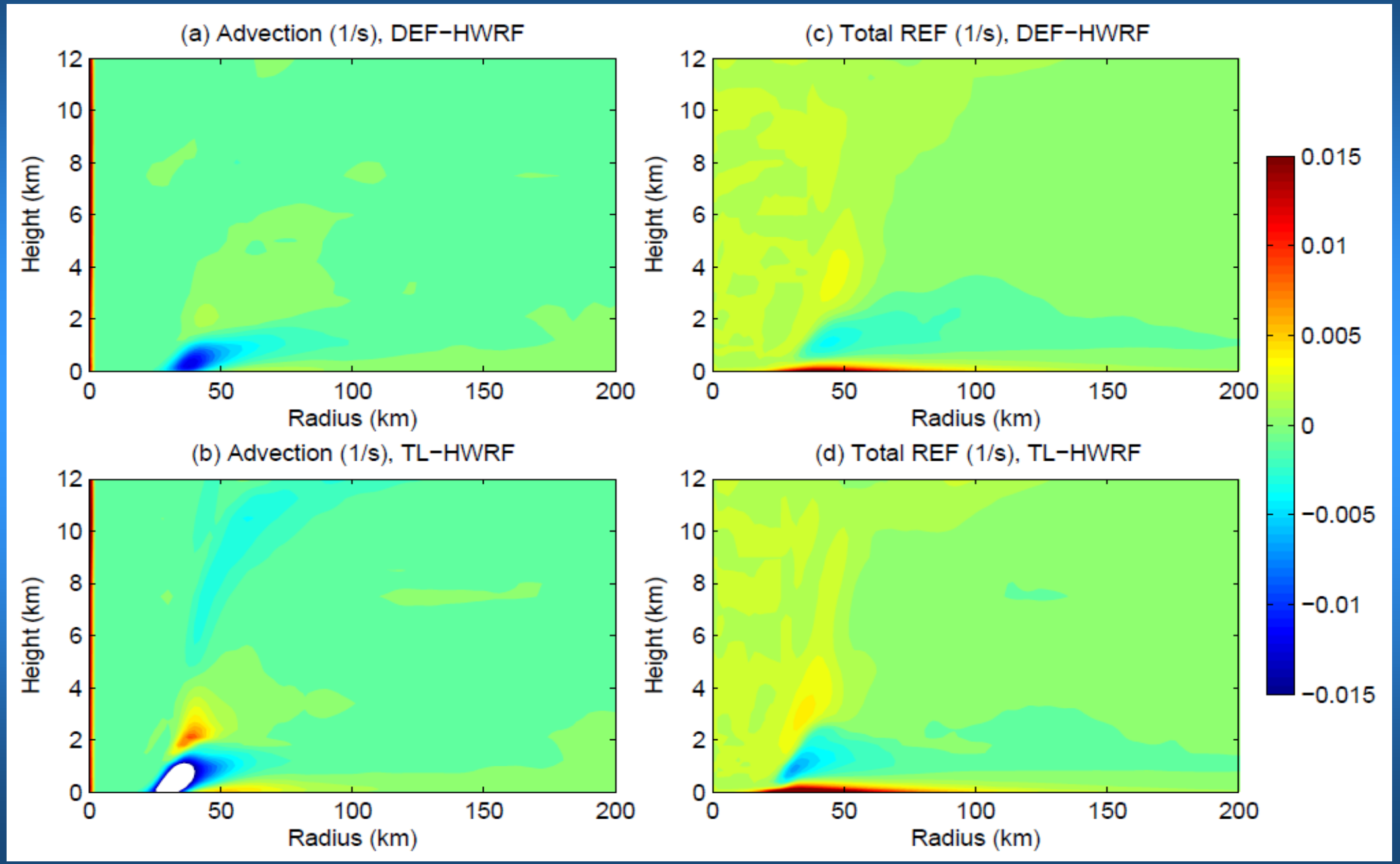

Sawyer-Eliassen diagnoses

$$C - \frac{1}{\bar{\rho}}\frac{\partial \bar{p}}{\partial r} = 0 \qquad -\frac{1}{\bar{\rho}}\frac{\partial \bar{p}}{\partial z} - g = 0 \longrightarrow \qquad g\frac{\partial \bar{\chi}}{\partial r} + \frac{\partial (C\bar{\chi})}{\partial z} = 0, \qquad \bar{\chi} = \frac{1}{\bar{\theta}}$$

Thermal wind relation: $$g\frac{\partial}{\partial r}\frac{\partial \bar{\chi}}{\partial t} + \frac{\partial}{\partial z}\frac{\partial (C\bar{\chi})}{\partial t} = 0$$

$$\frac{\partial \bar{\chi}}{\partial t} + \bar{u}\frac{\partial \bar{\chi}}{\partial r} + \bar{w}\frac{\partial \bar{\chi}}{\partial z} = -\bar{\chi}^2 Q, \qquad Q = \dot{\theta} + F_\theta + F_{sgs\_\theta}$$

$$\frac{\partial C}{\partial t} = \left(\frac{2\bar{v}}{r} + f\right)\frac{\partial \bar{v}}{\partial t}, \qquad \frac{\partial \bar{v}}{\partial t} = -\bar{u}\frac{\partial \bar{v}}{\partial r} - \bar{w}\frac{\partial \bar{v}}{\partial z} - \bar{u}\left(f + \frac{\bar{v}}{r}\right) + F_\lambda + F_{sgs_\lambda}$$

Stream function: $$\bar{u} = -\frac{1}{r\bar{\rho}}\frac{\partial \bar{\psi}}{\partial z}, \qquad \bar{w} = \frac{1}{r\bar{\rho}}\frac{\partial \bar{\psi}}{\partial r}$$

Sawyer-Eliassen Equation: $$A_{rr}\frac{\partial^2 \bar{\psi}}{\partial r^2} + A_{rz}\frac{\partial^2 \bar{\psi}}{\partial r \partial z} + A_{zz}\frac{\partial^2 \bar{\psi}}{\partial z^2} + A_r\frac{\partial \bar{\psi}}{\partial r} + A_z\frac{\partial \bar{\psi}}{\partial z} + A\bar{\psi} = R(r,z)$$

$$A_{rr}(r,z) = -g\frac{1}{r\bar{\rho}}\frac{\partial \bar{\chi}}{\partial z}, \qquad A_{rz}(r,z) = -\frac{2}{r\bar{\rho}}\frac{\partial (C\bar{\chi})}{\partial z}, \qquad A_{zz}(r,z) = \frac{1}{r\bar{\rho}}\left(\bar{\chi}\xi(f+\zeta) + C\frac{\partial \bar{\chi}}{\partial r}\right),$$

$$A_r(r,z) = \frac{\partial}{\partial r}\left(-\frac{g}{r\bar{\rho}}\frac{\partial \bar{\chi}}{\partial z}\right) + \frac{\partial}{\partial z}\left[-\frac{1}{r\bar{\rho}}\frac{\partial (C\bar{\chi})}{\partial z}\right], \qquad A_z(r,z) = \frac{\partial}{\partial r}\left[-\frac{1}{r\bar{\rho}}\frac{\partial (C\bar{\chi})}{\partial z}\right] + \frac{\partial}{\partial z}\left[\frac{1}{r\bar{\rho}}\left(\bar{\chi}\xi(f+\zeta) + C\frac{\partial \bar{\chi}}{\partial r}\right)\right], \qquad \mathrm{A}(r,z) = 0,$$

$$R(r,z) = g\frac{\partial}{\partial r}(\bar{\chi}^2 Q) + \frac{\partial}{\partial z}(C\bar{\chi}^2 Q) - \frac{\partial}{\partial z}\left[\bar{\chi}\xi\left(F_\lambda + F_{sgs_\lambda}\right)\right], \qquad \xi = f + \frac{2\bar{v}}{r}, \qquad \zeta = \frac{\bar{v}}{r} + \frac{\partial \bar{v}}{\partial r}.$$

Radial wind equation: $$U_{adv} - C = -\frac{1}{\bar{\rho}}\frac{\partial \bar{p}}{\partial r} = F_R, \qquad F_R = F_r + F_{sgs_r}, \qquad U_{adv} = \bar{u}\frac{\partial \bar{u}}{\partial r} + \bar{w}\frac{\partial \bar{u}}{\partial z}$$

Thermal wind-like relation: $$g\frac{\partial \bar{\chi}}{\partial r} + \frac{\partial[\bar{\chi}(C + F_R - U_{adv})]}{\partial z} = 0$$

Sawyer-Eliassen-like Equation: $$B_{rr}\frac{\partial^2 \bar{\psi}}{\partial r^2} + B_{rz}\frac{\partial^2 \bar{\psi}}{\partial r \partial z} + B_{zz}\frac{\partial^2 \bar{\psi}}{\partial z^2} + B_r\frac{\partial \bar{\psi}}{\partial r} + B_z\frac{\partial \bar{\psi}}{\partial z} + B\bar{\psi} = \mathrm{S}(r,z)$$

$$B_{rr}(r,z) = -g\frac{1}{r\bar{\rho}}\frac{\partial \bar{\chi}}{\partial z}, \qquad B_{rz}(r,z) = -\frac{1}{r\bar{\rho}}\left[2\frac{\partial(C\bar{\chi})}{\partial z} + \frac{\partial[(F_R - U_{adv})\bar{\chi}]}{\partial z} + (F_R - U_{adv})\frac{\partial \bar{\chi}}{\partial z}\right],$$

$$B_{zz}(r,z) = \frac{1}{r\bar{\rho}}\left[\bar{\chi}\xi(f+\zeta) + C\frac{\partial \bar{\chi}}{\partial r} + (F_R - U_{adv})\frac{\partial \bar{\chi}}{\partial r}\right],$$

$$B_r(r,z) = \frac{\partial}{\partial r}\left(-\frac{g}{r\bar{\rho}}\frac{\partial \bar{\chi}}{\partial z}\right) + \frac{\partial}{\partial z}\left[-\frac{1}{r\bar{\rho}}\frac{\partial(C\bar{\chi})}{\partial z}\right] - \frac{\partial}{\partial z}\left[\frac{(F_R - U_{adv})}{r\bar{\rho}}\frac{\partial \bar{\chi}}{\partial z}\right],$$

$$B_z(r,z) = \frac{\partial}{\partial r}\left[-\frac{1}{r\bar{\rho}}\frac{\partial(C\bar{\chi})}{\partial z}\right] + \frac{\partial}{\partial z}\left[\frac{1}{r\bar{\rho}}\left(\bar{\chi}\xi(f+\zeta) + C\frac{\partial \bar{\chi}}{\partial r}\right)\right] - \frac{\partial}{\partial r}\left[\frac{1}{r\bar{\rho}}\frac{\partial[(F_R - U_{adv})\bar{\chi}]}{\partial z}\right] + \frac{\partial}{\partial z}\left[\frac{(F_R - U_{adv})}{r\bar{\rho}}\frac{\partial \bar{\chi}}{\partial r}\right],$$

$$\mathrm{B}(r,z) = 0,$$

$$\mathrm{S}(r,z) = g\frac{\partial}{\partial r}(\bar{\chi}^2 Q) + \frac{\partial}{\partial z}(C\bar{\chi}^2 Q) - \frac{\partial}{\partial z}\left[\bar{\chi}\xi\left(F_\lambda + F_{sgs_\lambda}\right)\right] + \frac{\partial}{\partial z}\left[(F_R - U_{adv})\bar{\chi}^2 Q - \bar{\chi}\frac{\partial(F_R - U_{adv})}{\partial t}\right],$$

HWRF-DEF

HWRF-TL

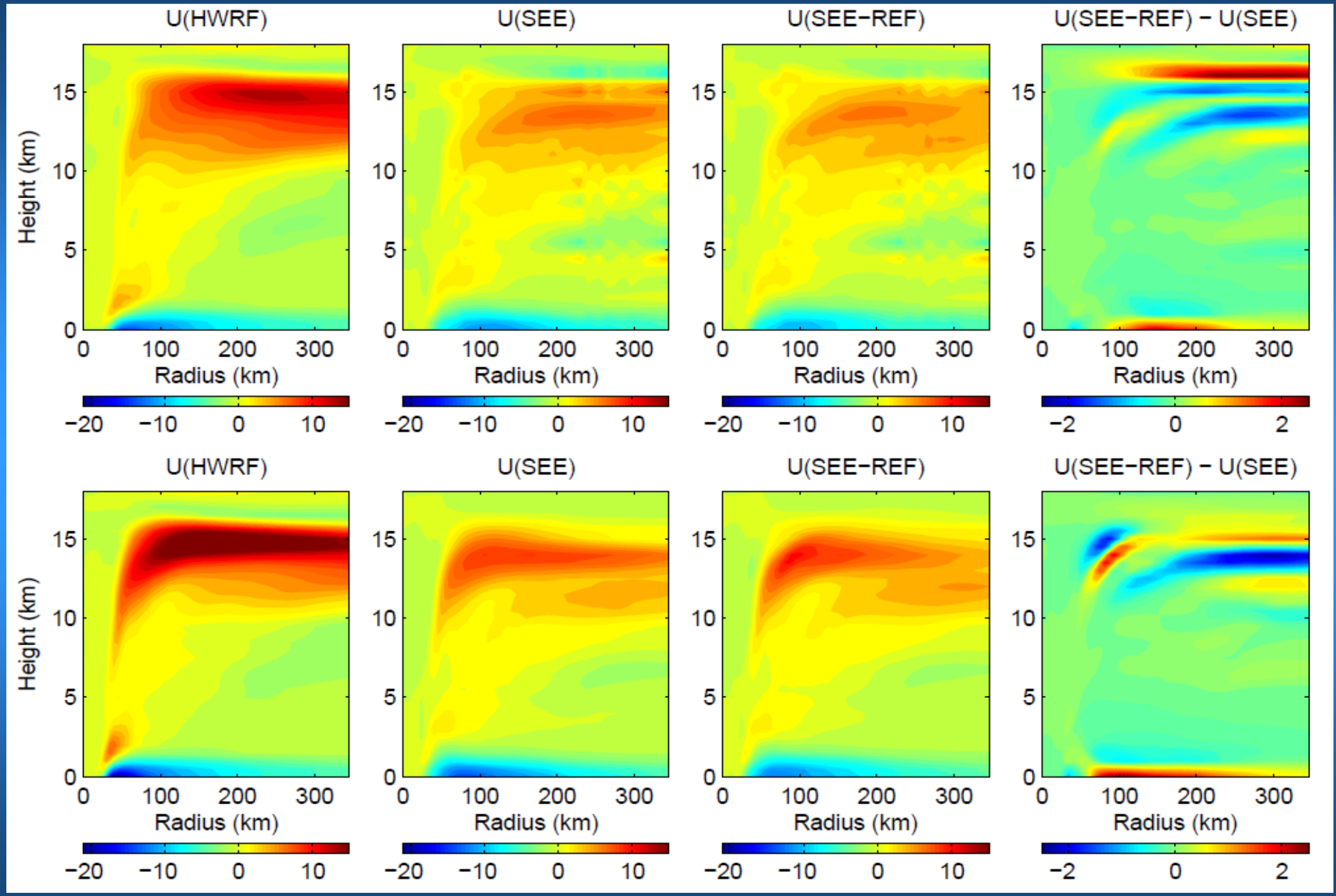

HWRF-DEF

HWRF-TL

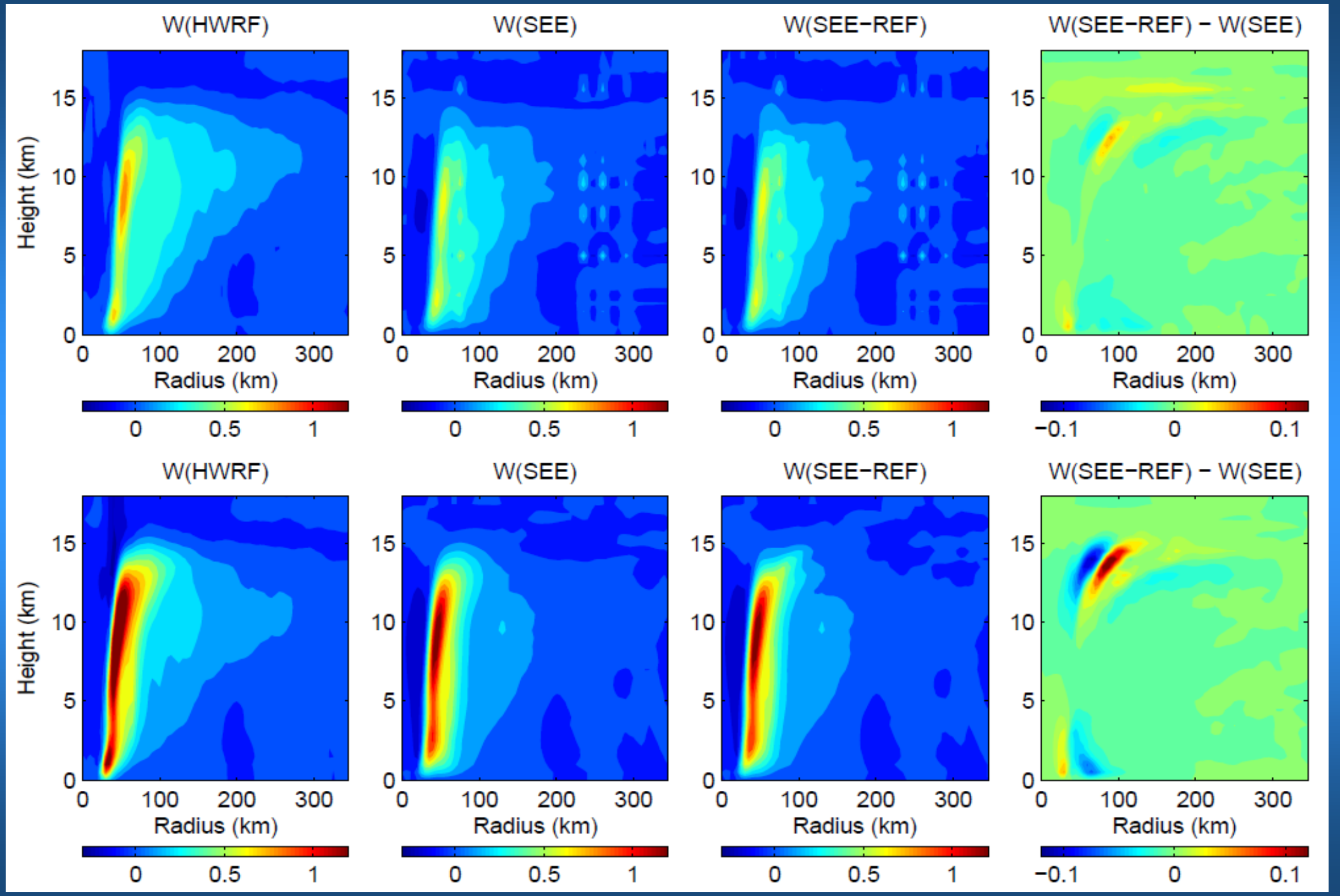

Summary

- A successful prediction of TC intensity depends on the skills of a model to generate eddy forcing that drives the primary and secondary circulations of a TC, provided that the model simulates correct large-scale fields and SST.
- While it is negative definite in the PBL, the sign of eddy forcing associated with eyewall/rainband convection above the PBL is indefinite. It can be positive depending on the detailed eddy processes, and thus, provides a mechanism to spin up a TC vortex.
- In numerical models, the continuous eyewall/rainband eddy forcing is artificially split into two parts: the model-resolved and SGS components, but they are not independent. While higher model resolution allows the eddy forcing to be better resolved, the SGS eddy forcing is a source of uncertainty. At the resolution of operational HWRF, the resolved eddy forcing and the associated storm inner-core structure show a substantial dependence on the SGS eddy forcing.
- With the correct determination of Brunt-Vaisala frequency in the clouds, the HWRF PBL scheme is shown to have the ability to appropriately generate in-cloud turbulent mixing in the eyewall and rainbands.
- We developed a SEE-like diagnostic equation that allows us to quantify the contributions of different components of forcing including tangential and radial eddy forcing to TC intensification.